THE ASTROPHYSICAL JOURNAL, 564:576–580, 2002 January 10

RADIO FOREGROUNDS FOR THE 21 CENTIMETER TOMOGRAPHY OF THE NEUTRAL INTERGALACTIC MEDIUM AT HIGH REDSHIFTS

TIZIANA DI MATTEO,[1,2] ROSALBA PERNA,[1,3] TOM ABEL,[1,4] AND MARTIN J. REES[4]

Received 2001 July 12; accepted 2001 September 11

ABSTRACT

Absorption or emission against the cosmic microwave background (CMB) radiation may be observed in the redshifted 21 cm line if the spin temperature of the neutral intergalactic medium (IGM) prior to reionization differs from the CMB temperature. This so-called 21 cm tomography should reveal important information on the physical state of the IGM at high redshifts. The fluctuations in the redshifted 21 cm line, due to gas density inhomogeneities at early times, should be observed at meter wavelengths by the next-generation radio telescopes such as the proposed Square Kilometer Array (SKA). Here we show that the extragalactic radio sources provide a serious contamination to the brightness temperature fluctuations expected in the redshifted 21 cm emission from the IGM at high redshifts. Unless the radio source population cuts off at flux levels above the planned sensitivity of SKA, its clustering noise component will dominate the angular fluctuations in the 21 cm signal. The integrated foreground signal is smooth in frequency space, and it should nonetheless be possible to identify the sharp spectral feature arising from the nonuniformities in the neutral hydrogen density during the epoch when the first UV sources reionize the IGM.

Subject headings: early universe — galaxies: general

1. INTRODUCTION

Studies of the Lyα forest in the spectra of high-redshift quasars have now clearly established that the universe is highly ionized by $z \sim 6$ and that the intergalactic medium (IGM) developed extensive nonlinear structures at these high redshifts. Although it is now possible to simulate the formation of the first ionizing objects in the universe (Gnedin & Ostriker 1997; Abel, Norman, & Madau 1999; Abel, Bryan, & Norman 2000; Gnedin 2000; Gnedin & Abel 2001), the epoch at which these objects were formed, their nature, and the timescale over which the transition from the neutral to the reionized universe occurs are currently unknown.

Building on the pioneering work of Field (1958, 1959) and Scott & Rees (1990), Madau, Meiksin, & Rees (1997, hereafter MMR97) proposed that 21 cm tomography can probe the IGM prior to the epoch of full reionization ($z > 6$). The idea is that the radiation from the first discrete sources should be detected indirectly through its interaction with the surrounding neutral IGM and in the resulting emission and/or absorption against the cosmic microwave background (CMB) at the frequency corresponding to the redshifted 21 cm line. The resulting patchwork (both in angle and in frequency) in the 21 cm radiation resulting from nonuniformities in the distribution of gas density and in the distribution of Lyα sources (i.e., the "cosmic web" at these early times) should be measurable with the next generation of radio telescopes (e.g., Tozzi et al. 2000; hereafter T00) such as the proposed Square Kilometer Array (SKA)[5] or the Low Frequency Array.[6]

In this paper, we assess the extent to which the detection of the redshifted 21 cm emission fluctuations is impeded by confusion noise from extragalactic foreground radio sources. In the following section we briefly summarize the physical origin and expected magnitude of the 21 cm signature. In § 3 we describe the extragalactic radio foreground emission and calculate its expected confusion noise component. Finally, in §§ 4 and 5 we present and discuss our results.

2. THE EXPECTED SIGNAL

Detailed investigations of the absorption/emission signal expected in the 21 cm radiation have been carried out by MMR97 and T00. It is anticipated that a strong soft UV background radiation field is established by the first stars and quasars prior to reionization (e.g., Haiman, Abel, & Rees 2000). Lyα photons from this background will couple the spin temperature of the neutral IGM to its kinetic gas temperature predominantly via the Wouthuysen-Field effect (Wouthuysen 1952; Field 1958). Since the IGM thermally decouples from the CMB at redshift ~ 130 and cools adiabatically thereafter [$T_{\rm IGM} \propto (1+z)^2$], one finds that $T_{\rm IGM}/T_{\rm CMB} \ll 1$ before the first luminous objects reheat the universe. Here the signal is in absorption against the CMB, and it is expected at the wavelength of 21 cm $\times (1 + z_{\rm Ly\alpha})$, where $z_{\rm Ly\alpha}$ denotes the redshift at which the spin temperature is first coupled to the kinetic gas temperature. Once the IGM is heated to a temperature above that of the CMB, the signal will be in emission and roughly independent of the spin temperature. The differential antenna temperature [the brightness temperature $T_B = T_{\rm CMB}\, e^{-\tau} + T_S\,(1 - e^{-\tau})$] observed at Earth between such a patch of IGM at a spin temperature T_S and the CMB is approximately given by (T00)

$$\langle \delta T^2 \rangle^{1/2} \approx 10 \text{ mK } h^{-1} \left(\frac{\Omega_B h^2}{0.02}\right) \left(\frac{1+z}{9}\right)^{1/2} \left(1 - \frac{T_{\rm CMB}}{T_S}\right), \quad (1)$$

[1] Harvard Smithsonian Center for Astrophysics, 60 Garden Street, Cambridge, MA 02138.
[2] *Chandra* Fellow.
[3] Harvard Junior Fellow.
[4] Institute of Astronomy, Madingley Road, Cambridge, CB03 0HA, UK.
[5] Additional information is available at http://www.nfra.nl/skai.
[6] Additional information is available at http://www.astron.nl/lofar.

where h denotes the current Hubble constant in units of 100 km s^{-1} Mpc^{-1} and Ω_B gives the baryon density in units of the critical density, while $|\delta T|$ is larger by a factor $T_{\rm CMB}/T_S$ ($\lesssim 18$ for reionization redshifts >6) for the absorption signal than for emission. Unfortunately, a relatively large radiation flux in Lyα is required to ensure the coupling of the spin temperature to the kinetic gas temperature. Therefore, the recoil from Lyα scatterings most likely heats the IGM to or above the CMB temperature before a sufficient Lyα background flux is established (MMR97). Consequently, the largest signals predicted by T00 and MMR97 are $\lesssim 10$ mK (at, e.g., 150 MHz if $z \sim 9$), as expected from equation (1), and the cosmic web at these times is most likely to be probed in emission at 21 cm. The appropriate resolution for measuring fluctuations in the IGM is of the order of 1′ with the frequency window of 1 MHz around 150 MHz (MMR97; T00). However, if the absorption feature was observed, it would give valuable insights into the epoch in which the first stars formed (MMR97; T00). At the epoch of reionization "breakthrough," the 21 cm signal from diffuse gas decreases steeply. One should be able to observe this signal integrated over most of the sky even with moderate instruments (Shaver et al. 1999). In the following sections we examine the confusion noise introduced at 150 MHz by extragalactic radio sources, and we discuss how this might impose serious limitations on the 21 cm tomography.

3. EXTRAGALACTIC RADIO FOREGROUNDS

SKA is planned to operate in the frequency range 0.01–20 GHz with an angular resolution of about 1″–10″ and a sensitivity down to a few tens of nanojanskys. Limitations on the sensitivity achievable for the measurement of the redshifted 21 cm signal will be set by the contamination from the galactic and extragalactic foregrounds. The dominant Galactic contribution is the synchrotron background, which comprises a fraction of about 70% at 150 MHz. On the angular scales that are most relevant for the 21 cm tomography, we nonetheless expect the dominant angular fluctuations to be caused by clustering and discreteness of extragalactic sources (discussed below).

The galactic foreground could only make a comparable contribution on subarcminute scales if throughout the interstellar medium and galactic halo there were fluctuations on the order of unity in its volume emissivity. Such fluctuations would exist, but only in small regions (e.g., active supernova remnants). On larger angular scales, where the galactic foreground fluctuations would be relatively more important, it has been sufficiently well studied (although at much higher radio frequencies than considered here) because of its importance for the observations of the CMB radiation (see references in Tegmark & Efstathiou 1996). A detailed discussion of the Galactic spectral contamination of the redshifted 21 cm is given in Shaver et al. (1999).

Detailed multiwavelength observations of the Galactic radio emission could be modeled with sufficient accuracy for our purpose (at least in some regions of the sky where observations would then take place). Hence, we limit our discussion to the confusion noise introduced by extragalactic foreground sources such as radio galaxies, active galactic nuclei, and normal galaxies that are likely to dominate the radio counts at the low flux density levels.

3.1. *Counts of Radio Sources at Low Radio Frequencies*

The wavelength region of interest is from 50 MHz ($z \sim 30$) to 200 MHz ($z \sim 6$). To evaluate the impact of extragalactic foreground radio sources in this wavelength range, it is necessary to model the number density of sources as a function of flux [the differential counts $N(S)$ per steradian]. At present, the appearance of the radio sky at flux-density levels below 1 μJy is not well known. However, deep Very Large Array (VLA) surveys have allowed one to extend direct determinations of radio source counts down to a few microjanskys (at $\nu \gtrsim 1.4$ GHz), implying a coverage of about 7 orders of magnitude in flux. At lower frequencies the limiting flux densities are higher because of the confusion noise introduced by extended sources.

The source counts from the 6C survey (Hales, Baldwin, & Warner 1988), which was carried out at 151 MHz, are a useful guide. The radio source counts at all frequencies are typically well described by a Euclidean power-law region at the highest flux densities, followed by a flatter portion at lower flux densities (e.g., Formalont et al. 1991). We therefore extrapolate the 151 MHz differential source counts by a double power law fitted to the observed counts. This gives

$$N(S) = \begin{cases} k_1 S^{-\gamma_1}, & S < S_0, \\ k_2 S^{-\gamma_2}, & S > S_0, \end{cases} \tag{2}$$

where $\gamma_1 = 1.75$, $\gamma_2 = 2.51$, and $k_1 = k_2 S_0^{\gamma_2 - \gamma_1}$, with $k_2 = 4.0\ \mathrm{sr}^{-1}\ \mathrm{mJy}^{-1}$ and $S_0 = 880$ mJy.

This fit also includes the counts from the 3CR survey and the 3CRR catalog at 178 MHz (Laing, Riley, & Longair 1983) transposed to 151 MHz, assuming a mean spectral index $\alpha = 0.75$ ($S \propto \nu^{-\alpha}$), typical for the emission from extended lobes at these frequencies (e.g., Laing et al. 1983). The limiting flux density for these surveys was ~ 100 mJy, and our extrapolation is somewhat uncertain. However, we will show that our main conclusions are insensitive to the particular choice of the source counts.

3.2. *Sky Fluctuations from Unresolved Sources*

The contribution to CMB fluctuations from randomly distributed sources of various natures has been extensively discussed in the literature (e.g., Scheuer 1974; Cavaliere & Setti 1976; Franceschini, Vercellone, & Fabian 1998; Tegmark & Efstathiou 1996; Scott & White 1998; Toffolatti et al. 1998; Perna & Di Matteo 2000). We can apply these techniques directly to the problem at hand. We estimate the confusion noise due to unidentified sources below a flux density limit $S_{\rm cut}$ that will contribute to fluctuations in the energy band of redshifted 21 cm emission. In the absence of clustering (Poisson distribution) the angular power spectrum, C_l, is a white noise ($C_l \sim$ constant). The contribution to the background below the flux cut $S_{\rm cut}$ due to sources with a Poisson distribution is given by

$$C_l^{\rm Poisson} = \langle S^2 \rangle = \int_0^{S_{\rm cut}} S^2 \frac{dN}{dS} dS\,. \tag{3}$$

However, the analysis of large samples of nearby radio galaxies has shown that sources are typically strongly clustered (e.g., Peacock & Nicholson 1991). Clustering decreases the effective number of objects in randomly distributed pixels and consequently enhances the pixel-to-pixel fluctuations (e.g., Peebles 1993). In the case of a power-law angular correlation function [$w(\theta) = (\theta/\theta_0)^{-\beta}$], the power

spectrum of intensity fluctuations due to clustered sources can be simply estimated as (e.g., Scott & White 1999)

$$C_l^{\rm cluster} = w_l I^2 , \quad (4)$$

where $w_l \propto l^{\beta-2}$ is the Legendre transform of $w(\theta)$ and $I = \int_0^{S_{\rm cut}} S(dN/dS)dS$ is the background contributed by sources below $S_{\rm cut}$. If sources are clustered like galaxies today or as Lyman break galaxies (Giavalisco et al. 1998) at $z \sim 3$, then we expect $\beta \approx 0.8 - 0.9$ (most of the sources at the faint flux density levels of interest here would in fact be galaxies). The angular correlation θ_0 is roughly independent of redshift because of the bias of high-redshift halos and is typically of the order of a few arcminutes (see, e.g., Oh 1999). Here we take $\theta_0 = 4'$.

We can compute the angular rms temperature fluctuation from

$$\langle T_{\rm rms}^2 \rangle^{1/2} = \left[\frac{l(l+1)C_l}{4\pi}\right]^{1/2} \left(\frac{\partial B_\nu}{\partial T}\right)^{-1} , \quad (5)$$

where

$$\frac{\partial B_\nu}{\partial T} = \frac{2k}{c^2}\left(\frac{kT}{h}\right)^2 \frac{x^4 e^x}{(e^x-1)^2} \quad (6)$$

is the conversion factor from temperature to flux density (per steradian), $B_\nu(T)$ is the Planck function, and $x \equiv h\nu/kT$, with $T = 2.725$ K (Mather et al. 1999) the CMB temperature. Note that the temperature fluctuations increase with increasing angular resolution.

4. CONFUSION NOISE

The rms brightness temperature fluctuation for various values of $S_{\rm cut}$ as a function of angular scale θ is shown in Figure 1. The thick lines represent the clustering term, and the thin lines represent the Poisson term.

The foreground signal from the point sources is typically larger than the 10 mK signal (eq. [1]) expected from the 21 cm radiation from the IGM at high redshifts. As expected, the signal decreases for decreasing values of $S_{\rm cut}$, i.e., if more sources can be identified and removed. In particular, as the value of the cutoff flux $S_{\rm cut}$ is lowered, the Poisson term declines much more sharply than the clustering term, until the latter totally dominates. Given our dN/dS, both components are dominated by objects just below the detection threshold $S_{\rm cut}$, but this dependence is stronger for the Poisson term. Thus, the subtraction of bright sources decreases the Poisson term much more effectively than the clustering term.

The SKA rms sensitivity is estimated to be (Rohls & Wilson 1996)[7]

$$S_{\rm instr} = \frac{2KT_{\rm sys}}{A_{\rm eff}\sqrt{2t\Delta\nu}} \sim 0.3\ \mu{\rm Jy}\left(\frac{1\ {\rm MHz}}{\Delta\nu}\right)^{1/2}\left(\frac{100\ {\rm hr}}{t}\right)^{1/2} \quad (7)$$

at 150 MHz. Therefore, in flux density units, the instrumental noise $S_{\rm instr}$ is independent of angular resolution. Given the appropriate angular resolution required to beat down source confusion, one can therefore identify and remove foreground sources down to flux densities of, e.g., $S_{\rm cut,\ lim} = 7S_{\rm instr}$. A limit on the angular resolution required to identify all sources down to $S_{\rm cut,\ lim}$ can be determined by comparing $S_{\rm cut,\ lim}$ to the confusion noise due to sources below this cutoff:

$$\frac{S}{N} \sim \frac{S_{\rm cut}}{(C_l^{\rm cluster}\|_{S_{\rm cut}}\theta^2)^{1/2}} \sim 10\left(\frac{S_{\rm cut}}{2.1\ \mu{\rm Jy}}\right)^{0.75}\left(\frac{\theta}{0''.3}\right)^{-1.55} . \quad (8)$$

Given that SKA is planned to achieve an angular resolution on the order of a fraction of an arcsecond, in principle it may be possible to remove all sources down to $S \sim S_{\rm cut,\ lim}$ without being limited by the confusion noise of the sources below that flux density. Figure 1 shows that even if sources are subtracted down to $S_{\rm cut} = 1\ \mu$Jy $\sim S_{\rm cut,\ lim}$, the foreground component (the Poisson component for $\theta < 10'$ and the clustering component for any θ) still dominates the primary 21 cm signal.

Note also that $S_{\rm cut,\ lim}$ will not be achieved if sources are even slightly extended, i.e., if their angular extent $\theta \gtrsim 0.3''$, which is a small number even at large distances. At these faint flux density levels, intrinsic source confusion due to their finite sizes would become important (see, e.g., Kellermann & Richards 1999).

These results clearly depend on the extrapolation of the radio source population (eq. [2]) down to flux density levels of the order of SKA sensitivity. Clearly, if the radio source population were to cutoff at flux densities above the SKA detection threshold, then all sources could be identified and removed, leaving no foreground contamination of the 21 cm signal.

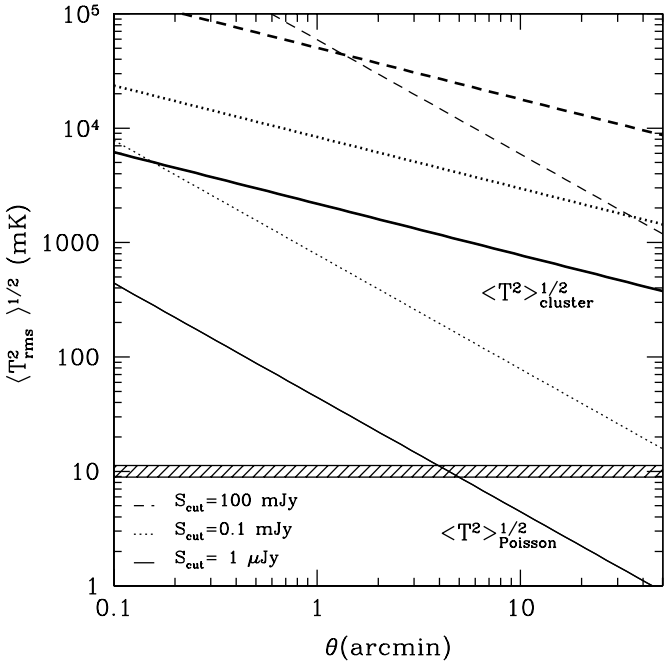

FIG. 1.—Angular dependence of the temperature fluctuations due to foreground sources at 150 MHz. Here the signal is shown after removal of all sources with flux densities $S > S_{\rm cut}$ as indicated in the figure. For each value of $S_{\rm cut}$, the thin lines show the Poisson noise, while the thick lines show the corresponding noise if the sources are clustered. For $S_{\rm cut} \lesssim 0.1$ mJy, the clustering term dominates the Poisson term at the scales of interest for the 21 cm observations. Note that the largest expected signal of 21 cm emission at high redshifts is below 10 mK, indicated by the hatched region.

[7] See also http://www.nfra.nl/skai/science.

However, this is unlikely given the typically shallow spectral slopes of radio sources and, in particular, the results from the deep VLA surveys, which found that radio counts at higher frequencies extend all the way down to the current instrumental sensitivities (e.g., at 5 GHz to flux densities ~ 1 μJy) without any evidence of a turnover. Indeed, VLA observations have revealed a further upturn of the differential counts of compact sources below a few microjanskys (Mitchell & Condon 1985; Windhorst et al. 1985), implying $N(\geq S) \propto S^{-1.2}$.

5. USING FREQUENCY INFORMATION

As we have seen in the previous section, within a realistic beam size one is integrating over a very large number of unresolved extragalactic sources. Their individual spectra are rather shallow, and typical observed flux densities of galaxies, supernovae remnants, the sky background, etc., scale with $\nu^{-\beta}$ with $0.8 < \beta < 0.2$ (Zombeck 1982). Hence, their integrated flux will also have a rather shallow slope. The 21 cm contribution, however, has steep spectral structures. The spectral index along a line of sight changes by an amount of the order of unity over a small frequency range $\Delta\nu$, where $\Delta\nu/\nu$ is the scale of neutral hydrogen nonuniformities relative to the Hubble radius. This change may occur multiple times along some lines of sight because of ionized regions prior to an ionization breakthrough. Subtracting out the measured power law of the foregrounds, one should see the leftover frequency dependence of the 21 cm contribution. Since the 21 cm signal is so sharp in frequency space, small errors in the measured integrated foreground spectrum will not hinder this measurement. For example, observing with 2 MHz resolution with an error of $\Delta\beta \sim 0.05$ of the measured foreground spectrum should allow one to distinguish a signal that is $(\nu/\nu_0)^{\Delta\beta} - 1 = (152/150)^{\Delta\beta} - 1 \sim 6 \times 10^{-4}$ times smaller than the foreground. Note that this argument assumes that the beam shape does not change for observations at a different frequency. Obviously, if the beam changes just slightly in size, then the clustering of the unresolved foregrounds will introduce noise in the spectra on the order of the change of area of the beam. However, it is not clear whether the large arrays needed to detect the signal will allow such good control over the synthesized beam, and a more detailed study of these technical limitations seems warranted. If these issues could be overcome, this signal would give very strong constraints on the nature of the sources reionizing the IGM. Not only could one pin down the epoch of reionization, but one could map the typical size of the regions of influence of individual sources.

6. CONCLUSIONS

Radio observations at meter wavelengths with instruments such as the SKA should map the large-scale structures at high redshift when the IGM had not yet been reionized ($6 \lesssim z \lesssim 30$). They should, therefore, provide a useful tool for probing the epoch, nature, and sources of reionization in the universe and their implications for cosmology.

Assuming that the radio Galactic foreground can be sufficiently modeled out (see Shaver et al. 1999 for possible strategies to do so), we have shown that the confusion noise provided by extragalactic radio sources provides a serious contamination to the brightness fluctuations expected in the redshifted 21 cm emission from the IGM at high redshifts. In particular, even if the radio source population is fully identified and removed down to the flux densities corresponding to the planned sensitivity of SKA, its clustering noise component will totally dominate the 21 cm signal at all scales and its Poisson component at scales $\theta < 10''$. Therefore, the detection of brightness fluctuations in the redshifted 21 cm seems unfeasible.

Note, however, that even in the case of significant foreground brightness fluctuations, the rise and decay of the 21 cm emission are expected to show very sharp features in frequency space that are potentially measurable even in the presence of the strong extragalactic (or Galactic) continuum. The integrated spectrum of extragalactic foreground sources will have a featureless power-law energy spectrum that will be measured directly and can be modeled out in frequency space. To detect the spectral deviations from the redshifted 21 cm signal, one would require observations in a sufficiently narrow bandwidth $\lesssim 5$ MHz. In particular, given such a narrow bandwidth, searching for the 21 cm signal should be possible even if there are spectral variations in the foregrounds. Any variation in frequency space in the foregrounds would be correlated (as the Galactic or extragalactic foreground have power-law spectra), whereas the 21 cm feature would appear as an uncorrelated signal and should therefore be detectable. Technical challenges as, e.g., techniques that minimize the change in the effective beam size as one changes the frequency band, will have to be addressed.

T. D. M. acknowledges partial support for this work provided by NASA through *Chandra* Postdoctoral Fellowship grant PF 8-10005 awarded by the *Chandra* Science Center, which is operated by the Smithsonian Astrophysical Observatory for NASA under contract NAS 8-39073 and support from grant NAG-10105. R. P. acknowledges support from Harvard Society of Fellows. T. A. acknowledges support from NSF grants ACI 96-19019 and AST 98-03137 and is grateful for many insightful discussions with Torsten Ensslin and Andreas Quirrenbach on radio observations.

REFERENCES

Abel, T., Bryan, G. L., & Norman, M. L. 2000, ApJ, 540, 39
Abel, T., Norman, M. L., & Madau, P. 1999, ApJ, 523, 66
Cavaliere, A., & Setti, G. 1976, A&A, 46, 81
Field, G. B. 1958, Proc. IRE, 46, 240
———. 1959, ApJ, 129, 536
Formalont, E. B., Windhorst, R. A., Kristian, J. A., & Kellerman, K. I. 1991, AJ, 102, 1258
Giavalisco, M., Steidel, C. C., Adelberger, K. L., Dickinson, M. E., Pettini, M., & Kellogg, M. 1998, ApJ, 503, 543
Gnedin, N. Y. 2000, ApJ, 535, 530
Gnedin, N. Y., & Abel, T. 2001, NewA, 6, 437
Gnedin, N. Y., & Ostriker, J. P. 1997, ApJ, 486, 581
Haiman, Z., Abel, T., & Rees, M. J. 2000, ApJ, 534, 11
Hales, S. E. G., Baldwin, J. E., & Warner, P. J. 1988, MNRAS, 234, 919
Kellermann, K. I., & Richards, E. A. 1999, in Perspectives on Radio Astronomy: Science with Large Antenna Arrays, ed. M. P. van Haarlem 1999 (Dwingeloo: ASTRON), 157
Laing, R. A., Riley, J. M., & Longair, M. S. 1983, MNRAS, 204, 151
Madau, P., Meiksin, A., & Rees, M. J. 1997, ApJ, 475, 429 (MMR97)
Mather, J. C., Fixsen, D. J., Shafer, R. A., Mosier, C., & Wilkinson, D. T. 1999, ApJ, 512, 511
Mitchell, K. J., & Condon, J. J. 1985, AJ, 90, 1957

Oh, S. P. 1999, ApJ, 527, 16
Peacock, J. A., & Nicholson, S. F. 1991, MNRAS, 253, 307
Peebles, P. J. E. 1993, Principles of Physical Cosmology (Princeton: Princeton Univ. Press)
Perna, R., & Di Matteo, T. 2000, ApJ, 542, 68
Razoumov, A. O., & Scott, D. 1999, MNRAS, 309, 287
Rohls, K., & Wilson, T. L. 1996, Tools of Radio Astronomy (Berlin: Springer)
Scheuer, P. A. G. 1974, MNRAS, 166, 329
Scott, D., & Rees, M. J. 1990, MNRAS, 247, 510
Scott, D., & White, M. 1999, A&A, 346, 1
Shaver, P. A., Windhorst, R. A., Madau, P., & de Bruyn, A. G. 1999, A&A, 345, 380
Tegmark, M., & Efstathiou, G. 1996, MNRAS, 281, 1297
Toffolatti, L., Gomez, F. A., De Zotti, G., Mazzei, P., Franceschini, A., Danese, L., & Burigana, C. 1998, MNRAS, 297, 117
Tozzi, P., Madau, P., Meiksin, A., & Rees, M. J. 2000, ApJ, 528, 597 (T00)
Windhorst, R. A., Miley, G. K., Owen, F. N., Kron, R. G., & Koo, D. C. 1985, ApJ, 289, 494
Wouthuysen, S. A. 1952, AJ, 57, 31
Zombeck, M. V. 1982, Handbook of Space Astronomy and Astrophysics (Cambridge: Cambridge Univ. Press)